

Supporting Material

Phosphatidylinositol-4,5-Bisphosphate (PIP₂) Stabilizes the Open Pore Conformation of the Kv11.1 (hERG) Channel

Nicolas Rodriguez, Mohamed Yassine Amarouch, Jérôme Montnach, Julien Piron, Alain J. Labro, Flavien Charpentier, Jean Mérot, Isabelle Baró, and Gildas Loussouarn

Supporting material

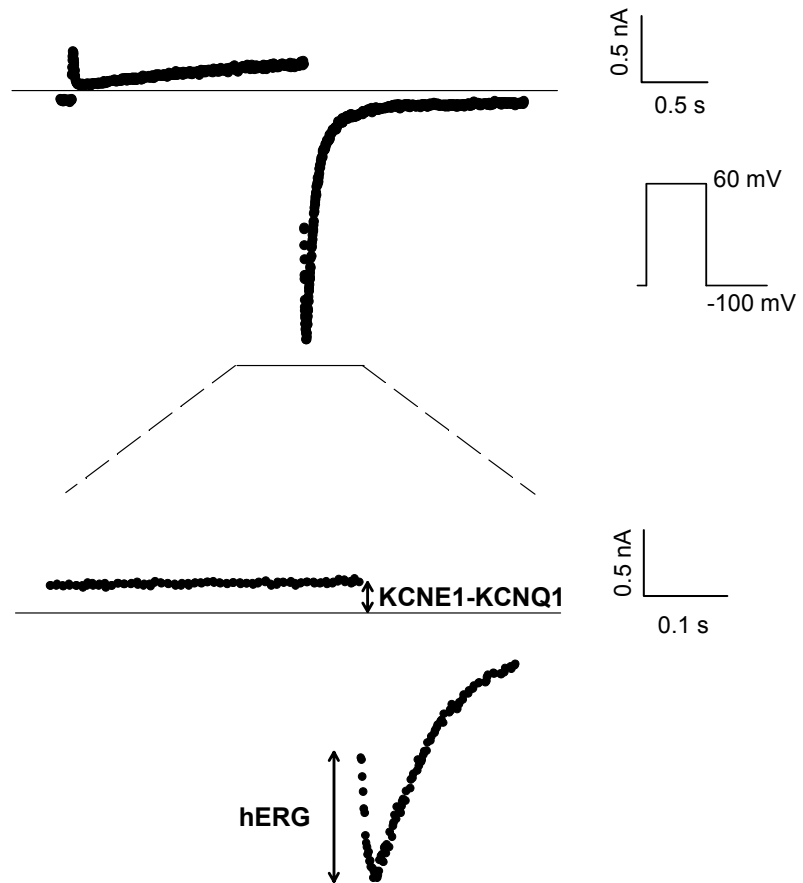


Figure S1. Determination of KCNE1-KCNQ1 and hERG currents from the co-transfection experiments. upper recording: current measured in response to a +60-mV step from a -100-mV holding potential, in a membrane patch of a co-transfected cell. Lower recording: magnification of the upper recording when the potential steps back from +60 mV to -100 mV. At the end of the +60 mV step, KCNE1-KCNQ1 is expected to be activated and hERG fully inactivated, so that the current recorded at the end of this pulse originates only from KCNE1-KCNQ1. On the other hand, KCNE1-KCNQ1 has no inactivation, so the recovery from inactivation observed after stepping back to -100 mV (hook) is due only to hERG channels.

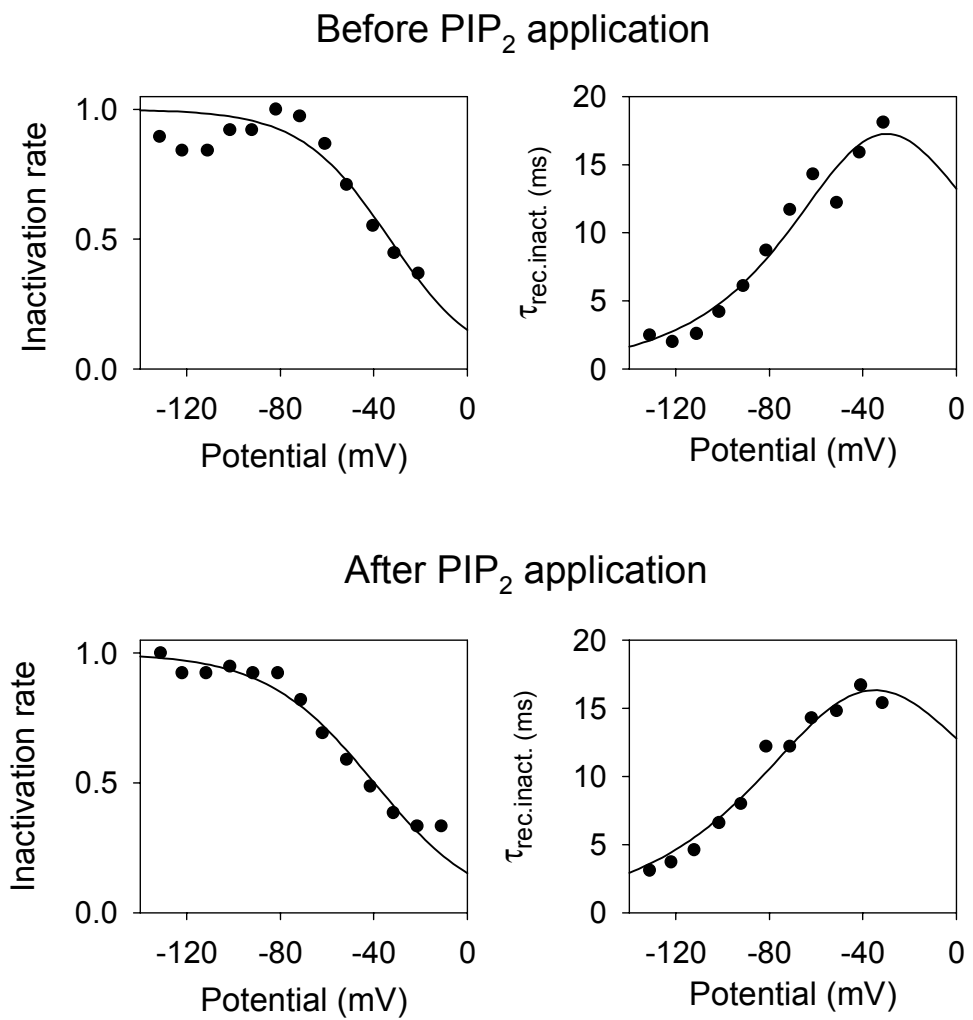


Figure S2. Determination of inactivation transition rates. To focus on activation properties, transition rates regarding inactivation of the models presented on figure 3 and figure S3 (α_l , β_l) are determined before and after PIP₂ addition from a concomitant fit of measured voltage-dependent inactivation rates and recovery from inactivation kinetics.

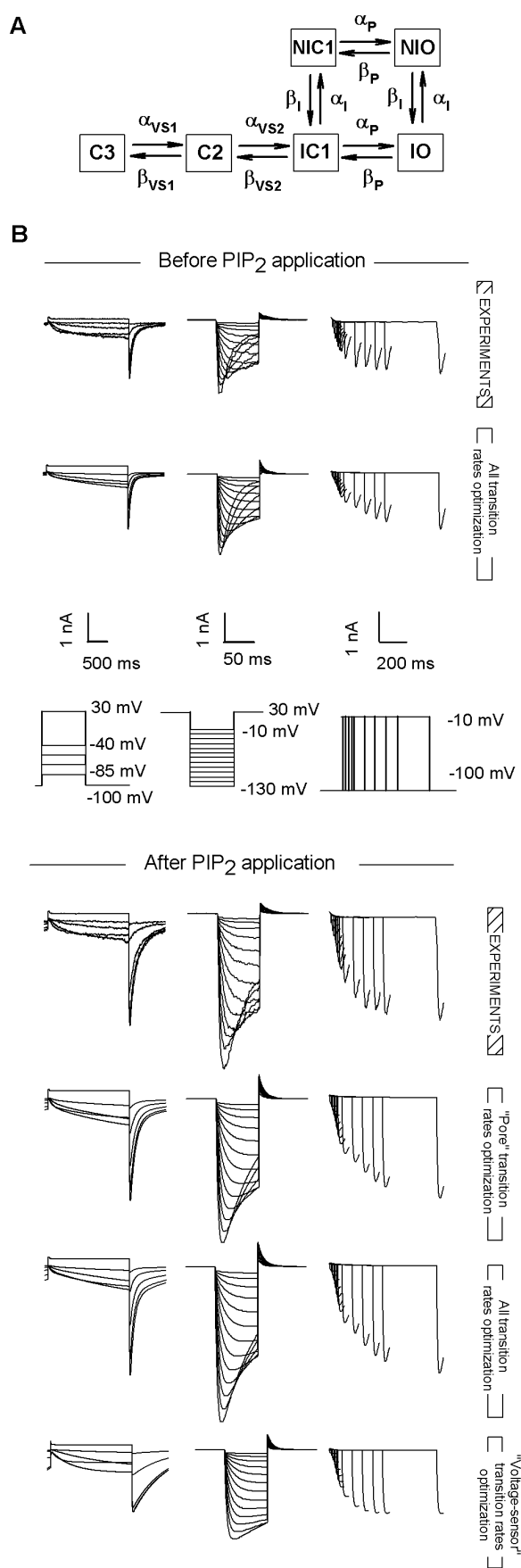


Figure S3. Weak activation/inactivation coupling kinetic model of hERG currents before and after PIP₂ application.

A: Kinetic model. Inactivation was modelled as a late transition that could occur from states IC1 or IO with the same transition rates. These rates were not optimized; they were determined from the fits of inactivation rate and the kinetics of recovery from inactivation (Fig. S2). The channel is open when it is in the NIO state. hERG current is given by $I = N.g.PNIO.(V_m - V_r)$. The late transitions (α_P, β_P) are voltage independent.

B: Simulation of hERG current time courses before and after PIP₂ application. Optimization of the late transitions (α_P, β_P), that are supposed to be related to the pore domain, lead to a reasonable fit of the PIP₂ effect, as good as the fit obtained by optimizing all transition rates. On the contrary, optimization of early voltage-dependent transition rates ($\alpha_{VS1}, \beta_{VS1}, \alpha_{VS2}, \beta_{VS2}$), that were supposed to be mainly related to the voltage sensing of hERG, lead to a poor fit of the PIP₂ effect. The transition rates and biophysical parameters determined from these simulations are shown on table S2. The results obtained from this kinetic model lead to the same conclusion as those obtained from the activation/inactivation uncoupled kinetic model of figure 3.

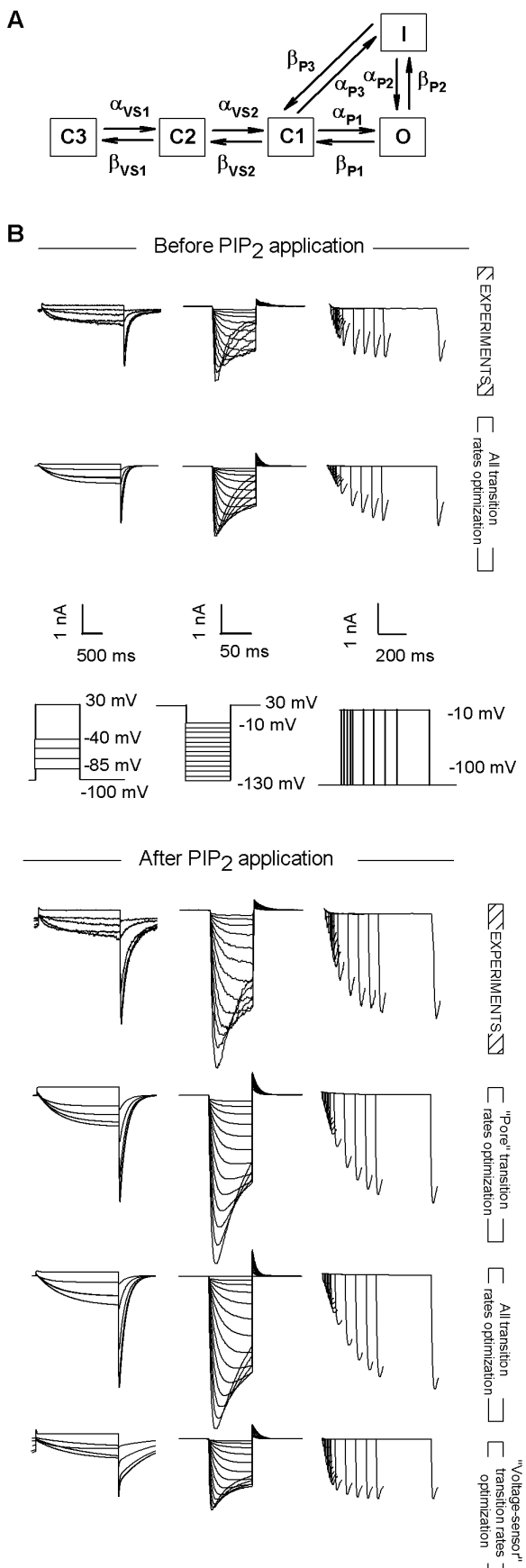
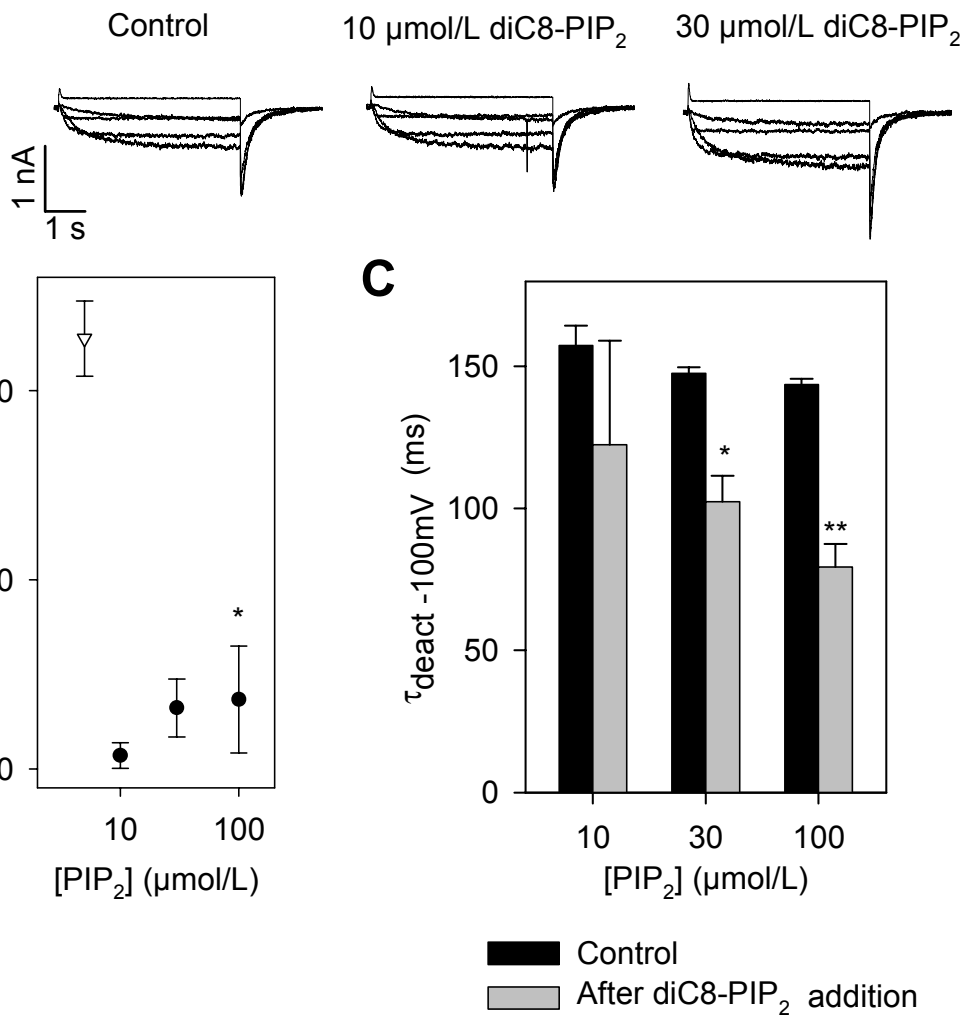


Figure S4. Activation/inactivation coupled kinetic model of hERG currents before and after PIP₂ application.

A: Kinetic model. This model is derived from previously used kinetic models of hERG (15). Inactivation was modelled as late transitions that are not independent from activation. All transition rates were voltage-dependent. Transition rates regarding inactivation were thus optimized and not determined independently in this case. The channel was open when it was in the O state. hERG current is given by $I = N.g.PO.(Vm-Vr)$.

B: Simulation of hERG current time courses before and after PIP₂ application. The optimization of the late transitions (α_{P1} , β_{P1} , α_{P2} , β_{P2} , α_{P3} , β_{P3}), that were supposed to be more related to the pore domain, lead to a reasonable fit of the PIP₂ effect, as good as the fit obtained by optimizing all transition rates. On the contrary, optimization of early voltage-dependent transition rates (α_{vs1} , β_{vs1} , α_{vs2} , β_{vs2}), that were supposed to be mainly related to the voltage sensing of hERG, lead to a poor fit of the PIP₂ effect. The transition rates and biophysical parameters determined from these simulations are shown on table S3. The results obtained from this kinetic model lead to the same conclusion as the one obtained from the activation/inactivation uncoupled kinetic model of figure 3.

A**Figure S5. diC8-PIP₂ dose response of hERG.**

A: Representative hERG current in absence (Control) and in the presence of 10 $\mu\text{mol/L}$ and 30 $\mu\text{mol/L}$ diC8-PIP₂. diC8-PIP₂ was applied to the cytosolic face of the patch, after current rundown. Same activation protocol as in figure 1. **B:** Relative increase, expressed in percentage, of the maximal tail current measured at -100 mV after a 1-s depolarization to +30 mV, as a function of diC8-PIP₂ concentration (black circle, N= 3-8). The downward triangle represents the effect of 5 $\mu\text{mol/L}$ PIP₂, for comparison. **C:** Deactivation time constants obtained from a monoexponential fit of the deactivating tail current before (control) and after diC8-PIP₂ application. (N= 3-8 cells). *: p<0.05, **:p<0.01.

Supplementary Tables

Table S1

		Before PIP ₂	After PIP ₂		
		$\alpha_{VS1}, \beta_{VS1}, \alpha_{VS2}, \beta_{VS2}, \alpha_P, \beta_P$ optimized	α_P, β_P optimized	$\alpha_{VS1}, \beta_{VS1}, \alpha_{VS2}, \beta_{VS2}, \alpha_P, \beta_P$ optimized	$\alpha_{VS1}, \beta_{VS1}, \alpha_{VS2}, \beta_{VS2}$ optimized
Transition rates	α_{VS1}	$5.09 \cdot 10^{-3} \exp(4.36 \cdot 10^{-2} \cdot v)$	$5.09 \cdot 10^{-3} \exp(4.36 \cdot 10^{-2} \cdot v)$	$7.02 \cdot 10^{-3} \exp(4.39 \cdot 10^{-2} \cdot v)$	$1.72 \cdot 10^{-2} \exp(2.48 \cdot 10^{-2} \cdot v)$
	β_{VS1}	$2.44 \cdot 10^{-4} \exp(-9.8 \cdot 10^{-2} \cdot v)$	$2.44 \cdot 10^{-4} \exp(-9.8 \cdot 10^{-2} \cdot v)$	$4.89 \cdot 10^{-4} \exp(-4.83 \cdot 10^{-2} \cdot v)$	$2.61 \cdot 10^{-5} \exp(-1.37 \cdot 10^{-1} \cdot v)$
	α_{VS2}	$6.73 \cdot 10^{-2} \exp(3.72 \cdot 10^{-2} \cdot v)$	$6.73 \cdot 10^{-2} \exp(3.72 \cdot 10^{-2} \cdot v)$	$4.98 \cdot 10^{-2} \exp(3.34 \cdot 10^{-2} \cdot v)$	$2.61 \cdot 10^{-2}$
	β_{VS2}	$5.21 \cdot 10^{-5} \exp(-6.2 \cdot 10^{-2} \cdot v)$	$5.21 \cdot 10^{-5} \exp(-6.2 \cdot 10^{-2} \cdot v)$	$7.76 \cdot 10^{-5} \exp(-6.42 \cdot 10^{-2} \cdot v)$	$2.96 \cdot 10^{-5} \exp(-4.29 \cdot 10^{-2} \cdot v)$
	α_P	$5.18 \cdot 10^{-2}$	$4.73 \cdot 10^{-2}$	$5.28 \cdot 10^{-2}$	$5.18 \cdot 10^{-2}$
	β_P	$8.07 \cdot 10^{-2}$	$2.07 \cdot 10^{-2}$	$1.74 \cdot 10^{-2}$	$8.07 \cdot 10^{-2}$
	α_I	$1.13 \cdot 10^{-2} \exp(-2.85 \cdot 10^{-2} \cdot v)$	$1.19 \cdot 10^{-2} \exp(-2.39 \cdot 10^{-2} \cdot v)$	$1.19 \cdot 10^{-2} \exp(-2.39 \cdot 10^{-2} \cdot v)$	$1.19 \cdot 10^{-2} \exp(-2.39 \cdot 10^{-2} \cdot v)$
	β_I	$6.43 \cdot 10^{-2} \exp(-2.39 \cdot 10^{-2} \cdot v)$	$6.64 \cdot 10^{-2} \exp(-1.93 \cdot 10^{-2} \cdot v)$	$6.64 \cdot 10^{-2} \exp(-1.93 \cdot 10^{-2} \cdot v)$	$6.64 \cdot 10^{-2} \exp(-1.93 \cdot 10^{-2} \cdot v)$
Biophysical parameters	Relat. max. current	1 (1)	1.7 (1.88)	1.78 (1.88)	1.03 (1.88)
	$\tau_{deac -100mV}$	64 ms (88)	140 ms (176)	122 ms (176)	718 ms (176)
	$V_{1/2\text{activation}}$	-64 mV (-64.5)	-64 mV (-63.1)	-63.6 mV (-63.1)	-64.8 mV (-63.1)
	$\tau_{act-55mV}$	625 ms (421)	637 ms (567)	763 ms (567)	728 ms (567)
	$\tau_{recov.inac -100mV}$	3.8 ms (3.9)	6.1 ms (6.0)	6.0 ms (6.0)	6.6 ms (6.0)
	$V_{1/2\text{inactiv.}}$	-28.2 mV (-28.6)	-33.4 mV (-40.5)	-32.7 mV (-40.5)	-36.9 mV (-40.5)

Table S2

		Before PIP ₂	After PIP ₂		
		$\alpha_{VS1}, \beta_{VS1}, \alpha_{VS2}, \beta_{VS2}, \alpha_P, \beta_P$ optimized	α_P, β_P optimized	$\alpha_{VS1}, \beta_{VS1}, \alpha_{VS2}, \beta_{VS2}, \alpha_P, \beta_P$ optimized	$\alpha_{VS1}, \beta_{VS1}, \alpha_{VS2}, \beta_{VS2}$ optimized
Transition rates	α_{VS1}	$5.15 \cdot 10^{-3} \exp(4.26 \cdot 10^{-2} \cdot v)$	$5.15 \cdot 10^{-3} \exp(4.26 \cdot 10^{-2} \cdot v)$	$6.77 \cdot 10^{-3} \exp(5.1 \cdot 10^{-2} \cdot v)$	$1.8 \cdot 10^{-2} \exp(1.66 \cdot 10^{-2} \cdot v)$
	β_{VS1}	$2.5 \cdot 10^{-3} \exp(-9.51 \cdot 10^{-3} \cdot v)$	$2.5 \cdot 10^{-3} \exp(-9.51 \cdot 10^{-3} \cdot v)$	$4.14 \cdot 10^{-4} \exp(-7.58 \cdot 10^{-3} \cdot v)$	$1.34 \cdot 10^{-3} \exp(-1.05 \cdot 10^{-1} \cdot v)$
	α_{VS2}	$7.09 \cdot 10^{-2} \exp(3.63 \cdot 10^{-2} \cdot v)$	$7.09 \cdot 10^{-2} \exp(3.63 \cdot 10^{-2} \cdot v)$	$6.29 \cdot 10^{-2} \exp(2.77 \cdot 10^{-2} \cdot v)$	$3.51 \cdot 10^{-2} \exp(9.76 \cdot 10^{-3} \cdot v)$
	β_{VS2}	$5.76 \cdot 10^{-5} \exp(-6.06 \cdot 10^{-2} \cdot v)$	$5.76 \cdot 10^{-5} \exp(-6.06 \cdot 10^{-2} \cdot v)$	$2.37 \cdot 10^{-4} \exp(-5.27 \cdot 10^{-2} \cdot v)$	$4.09 \cdot 10^{-5} \exp(-3.94 \cdot 10^{-2} \cdot v)$
	α_P	$6.61 \cdot 10^{-2}$	$5.02 \cdot 10^{-2}$	$5.54 \cdot 10^{-2}$	$6.61 \cdot 10^{-2}$
	β_P	$1.01 \cdot 10^{-1}$	$2.45 \cdot 10^{-2}$	$2.11 \cdot 10^{-2}$	$1.01 \cdot 10^{-1}$
	α_I	$1.13 \cdot 10^{-2} \exp(-2.85 \cdot 10^{-2} \cdot v)$	$1.19 \cdot 10^{-2} \exp(-2.39 \cdot 10^{-2} \cdot v)$	$1.19 \cdot 10^{-2} \exp(-2.39 \cdot 10^{-2} \cdot v)$	$1.19 \cdot 10^{-2} \exp(-2.39 \cdot 10^{-2} \cdot v)$
	β_I	$6.43 \cdot 10^{-2} \exp(-2.39 \cdot 10^{-2} \cdot v)$	$6.64 \cdot 10^{-2} \exp(-1.93 \cdot 10^{-2} \cdot v)$	$6.64 \cdot 10^{-2} \exp(-1.93 \cdot 10^{-2} \cdot v)$	$6.64 \cdot 10^{-2} \exp(-1.93 \cdot 10^{-2} \cdot v)$
Biophysical parameters	Relat. max. current	1 (1)	1.75 (1.88)	1.86 (1.88)	1.06 (1.88)
	$\tau_{deac -100mV}$	66 ms (88)	139 ms (176)	114 ms (176)	1020 ms (176)
	$V_{1/2\text{activation}}$	-63.9 mV (-64.5)	-65.3 mV (-63.1)	-59.7 mV (-63.1)	-70.5 mV (-63.1)
	$\tau_{act-55mV}$	623 ms (421)	655 ms (567)	989 ms (567)	579 ms (567)
	$\tau_{recov.inac -100mV}$	4.3 ms (3.9)	6.3 ms (6.0)	6.2 ms (6.0)	6.7 ms (6.0)
	$V_{1/2\text{inactiv.}}$	-27.7 mV (-28.6)	-34.5 mV (-40.5)	-34.3 mV (-40.5)	-37.9 mV (-40.5)

Table S3

		Before PIP ₂	After PIP ₂	
Transition rates	$\alpha_{VS1}, \beta_{VS1}, \alpha_{VS2}, \beta_{VS2}, \alpha_{P1}, \beta_{P1}, \alpha_{P2}, \beta_{P2}, \alpha_{P3}$ optimized	$\alpha_{P1}, \beta_{P1}, \alpha_{P2}, \beta_{P2}, \alpha_{P3}$ optimized	$\alpha_{VS1}, \beta_{VS1}, \alpha_{VS2}, \beta_{VS2}, \alpha_{P1}, \beta_{P1}, \alpha_{P2}, \beta_{P2}, \alpha_{P3}$ optimized	$\alpha_{VS1}, \beta_{VS1}, \alpha_{VS2}, \beta_{VS2}$ optimized
	α_{VS1}	$7.83 \cdot 10^{-1} \exp(4.09 \cdot 10^{-4} \cdot v)$	$7.83 \cdot 10^{-1} \exp(4.09 \cdot 10^{-4} \cdot v)$	$1.083 \exp(3.14 \cdot 10^{-4} \cdot v)$
	β_{VS1}	$8.58 \cdot 10^{-3} \exp(-9.24 \cdot 10^{-3} \cdot v)$	$8.58 \cdot 10^{-3} \exp(-9.24 \cdot 10^{-3} \cdot v)$	$2.45 \cdot 10^{-3} \exp(-1.02 \cdot 10^{-2} \cdot v)$
	α_{VS2}	$8.89 \cdot 10^{-3} \exp(2.96 \cdot 10^{-2} \cdot v)$	$8.89 \cdot 10^{-3} \exp(2.96 \cdot 10^{-2} \cdot v)$	$7.76 \cdot 10^{-3} \exp(3.49 \cdot 10^{-2} \cdot v)$
	β_{VS2}	$1.25 \cdot 10^{-4} \exp(-4.98 \cdot 10^{-2} \cdot v)$	$1.25 \cdot 10^{-4} \exp(-4.98 \cdot 10^{-2} \cdot v)$	$2.31 \cdot 10^{-4} \exp(-4.84 \cdot 10^{-2} \cdot v)$
	α_{P1}	$3.27 \cdot 10^{-2} \exp(1.09 \cdot 10^{-2} \cdot v)$	$6.23 \cdot 10^{-2} \exp(7.73 \cdot 10^{-3} \cdot v)$	$7.62 \cdot 10^{-2} \exp(5.13 \cdot 10^{-3} \cdot v)$
	β_{P1}	$1.75 \cdot 10^{-2} \exp(-6.32 \cdot 10^{-3} \cdot v)$	$1.41 \cdot 10^{-2} \exp(-3.84 \cdot 10^{-3} \cdot v)$	$1.52 \cdot 10^{-2} \exp(-2.05 \cdot 10^{-3} \cdot v)$
	α_{P2}	$3.19 \cdot 10^{-3} \exp(-3.15 \cdot 10^{-2} \cdot v)$	$1.04 \cdot 10^{-2} \exp(-2.18 \cdot 10^{-2} \cdot v)$	$5.68 \cdot 10^{-3} \exp(-2.7 \cdot 10^{-2} \cdot v)$
	β_{P2}	$9.05 \cdot 10^{-2} \exp(1.85 \cdot 10^{-2} \cdot v)$	$7.92 \cdot 10^{-2} \exp(1.37 \cdot 10^{-2} \cdot v)$	$8.66 \cdot 10^{-2} \exp(2.58 \cdot 10^{-2} \cdot v)$
	α_{P3}	$7.22 \cdot 10^{-2} \exp(2.27 \cdot 10^{-2} \cdot v)$	$7.83 \cdot 10^{-2} \exp(2.62 \cdot 10^{-2} \cdot v)$	$5.37 \cdot 10^{-2} \exp(2.32 \cdot 10^{-2} \cdot v)$
Biophysical parameters	Relat. max. current	1 (1)	1.93 (1.88)	1.97 (1.88)
	τ_{deac} -100mV	73 ms (88)	145 ms (176)	152 ms (176)
	$V_{1/2}$ activation	-65.4 mV (-64.5)	-69.3 mV (-63.1)	-63.7 mV (-63.1)
	τ_{act} -55mV	449 ms (421)	534 ms (567)	653 ms (567)
	$\tau_{recov.inac}$ -100mV	3.8 ms (3.9)	5.8 ms (6.0)	7.1 ms (6.0)
	$V_{1/2}$ inactiv.	-35.3 mV (-28.6)	-50.1 mV (-40.5)	-40 mV (-40.5)

S1: Transition rates and biophysical parameters corresponding to the model of figure 3. Biophysical parameters measured before and after PIP₂ addition on the cell used to optimize the transition rates are shown in brackets on the right of simulated values.

S2: Transition rates and biophysical parameters corresponding to the model of supplementary figure 3.

S3: Transition rates and biophysical parameters corresponding to the model of supplementary figure 4.